1116 *Inorg. Chem.* **2011**, *50*, 1116–1122
DOI: 10.1021/ic1023778

Inorganic Chemistry
Article

Magnesium Imide: Synthesis and Structure Determination of an Unconventional Alkaline Earth Imide from Decomposition of Magnesium Amide

Francesco Dolci,*,† Emilio Napolitano,‡ Eveline Weidner,† Stefano Enzo,‡ Pietro Moretto,† Michela Brunelli,§ Thomas Hansen,§ Maximilian Fichtner,∥ and Wiebke Lohstroh∥

†*Institute for Energy, DG Joint Research Centre, European Commission, P.O. Box 2, 1755 ZG Petten, The Netherlands,* ‡*Dipartimento di Chimica and INSTM, University of Sassari, via Vienna n. 2, I-07100 Sassari, Italy,* §*Institut Laue-Langevin, Rue Jules Horowitz 6, 38043, Grenoble, France, and* ∥*Institute of Nanotechnology, Karlsruhe Institute of Technology, Postfach 3640, 76021 Karlsruhe, Germany*

Received September 23, 2010

Magnesium imide (MgNH) was produced by monitoring the decomposition process of magnesium amide with in situ neutron diffraction. Significant changes in the structure of magnesium amide are detected during heat treatment and eventually result in the formation of crystalline MgNH. A model for the crystal structure of magnesium imide (MgNH) is presented for the first time. Remarkably, magnesium imide offers unique structural features similar to the cyclosilicate class and can be described as a porous solid formed by a sequence of linked chains of face sharing Mg_6N_6 hexagonal prism clusters.

1. Introduction

Alkali amide materials MNH_2 and alkaline earth analogues $M'(NH_2)_2$ (M: alkali metal, M′: alkaline earth metal) have been known for more than a century and a half,[1] and they are still subject to intense research nowadays.[2] Particularly, in 2002, the discovery that mixtures of lithium amide and lithium hydride could serve as solid state hydrogen storage materials, renewed the interest in this class of materials.[3] Since then, a variety of amide/hydride mixtures have been investigated.[4−9] The detailed knowledge of the structures and stabilities of the phases involved is considered a key step for the genesis and control of promising hydrogen storage materials. Recent studies focused on the interplay between reactivity and crystal structure for mixed amide/hydride systems.[7,10−12] Despite the considerable amount of work done both on the pure amides compounds and, more recently, on mixed amide/hydride systems, crystal structure models for many of these compounds are often unavailable.[10−16] However, this information is a mandatory prerequisite for the establishment of accurate full thermodynamic assessments.[17] In particular, the first paper containing a structural model on $Mg(NH_2)_2$[18] reported also the cell parameters of its solid decomposition product, MgNH, but its structure remained unsolved prior to this study. Many authors reported a parallelism between group I and II oxides and the respective imides.[7,10,19] Isotypical cubic structures are found for instance both for lithium, calcium, barium, and strontium; magnesium, however, does not seem to follow this trend.

*To whom correspondence should be addressed. E-mail: francesco.dolci@ec.europa.eu. Phone: +31-(0)22456-5261.

(1) Bergstrom, F. W.; Fernelius, W. C. *Chem. Rev.* **1937**, *20*, 413–481.
(2) Lappert, M.; Power, P.; Protchenko, A.; Seeber, A. *Metal Amide Chemistry*; Wiley: New York, 2009.
(3) Chen, P.; Xiong, Z.; Luo, J.; Lin, J.; Lee Tan, K. *Nature* **2002**, *420*, 302–304.
(4) Xiong, Z.; Wu, G.; Hu, J.; Chen, P. *Adv. Mater.* **2004**, *16*, 1522–1525.
(5) Balogh, M. P.; Jones, C. Y.; Herbst, J. F.; Hector, L. G., Jr; Kundrat, M. *J. Alloys Compd.* **2006**, *420*, 326–336.
(6) Orimo, S. I.; Nakamori, Y.; Eliseo, J. R.; Zuttel, A.; Jensen, C. M. *Chem. Rev.* **2007**, *107*, 4111–4132.
(7) David, W. I. F.; Jones, M. O.; Gregory, D. H.; Jewell, C. M.; Johnson, S. R.; Walton, A.; Edwards, P. P. *J. Am. Chem. Soc.* **2007**, *129*, 1594–1601.
(8) Lowton, R. L.; Jones, M. O.; David, W. I. F.; Johnson, S. R.; Sommariva, M.; Edwards, P. P. *J. Mater. Chem.* **2008**, *18*, 2355–2360.
(9) Gregory, D. H. *J. Mater. Chem.* **2008**, *18*, 2321–2330.
(10) Wu, H. *J. Am. Chem. Soc.* **2008**, *130*, 6515–6522.
(11) Weidner, E.; Bull, D. J.; Shabalin, I. L.; Keens, S. G.; Telling, M. T. F.; Ross, D. K. *Chem. Phys. Lett.* **2007**, *444*, 76–79.
(12) Rijssenbeek, J.; Gao, Y.; Hanson, J.; Huang, Q.; Jones, C.; Toby, B. *J. Alloys Compd.* **2008**, *454*, 233–244.
(13) Hu, J.; Liu, Y.; Wu, G.; Xiong, Z.; Chen, P. *J. Phys. Chem. C* **2007**, *111*, 18439–18443.
(14) Luo, W.; Sickafoose, S. *J. Alloys Compd.* **2006**, *407*, 274–281.
(15) Leng, H.; Ichikawa, T.; Fujii, H. *J. Phys. Chem. B* **2006**, *110*, 12964–12968.
(16) Weidner, E.; Dolci, F.; Hu, J.; Lohstroh, W.; Hansen, T.; Bull, D. J.; Fichtner, M. *J. Phys. Chem. C* **2009**, *113*, 15772–15777.
(17) Michel, K. J.; Akbarzadeh, A. R.; Ozolins, V. *J. Phys. Chem. C* **2009**, *113*, 14551–14558.
(18) Jacobs, H.; Juza, R. *Z. Anorg. Allg. Chem.* **1969**, *370*, 254–261.
(19) Juza, R. *Angew. Chem., Int. Ed.* **1964**, *3*, 471–481.

 Published on Web 12/29/2010

The common decomposition reaction pathway evidenced for every alkali and alkaline earth amide material is[20,21]

$$2MNH_2 \rightarrow M_2NH + NH_3 \quad (1a)$$

$$3M_2NH \rightarrow 2M_3N + NH_3 \quad (2a)$$

$$M'(NH_2)_2 \rightarrow M'NH + NH_3 \quad (1b)$$

$$3M'NH \rightarrow M'_3N_2 + NH_3 \quad (2b)$$

where M is a group I metal, and M′ is a group II metal. Accordingly, magnesium amide, under thermal treatment, follows the analogous process: first ammonia is released forming the imide and then is further released upon nitride formation. One difficulty in the preparation of a pure MgNH phase by thermal decomposition from $Mg(NH_2)_2$ appears to be the relative instability of MgNH against magnesium nitride (Mg_3N_2) formation. This is why, in this study the in situ neutron diffraction technique was used to directly monitor in real time the thermal decomposition of magnesium amide to magnesium imide.

2. Experimental Section

Deuterated magnesium amide ($Mg(ND_2)_2$) was prepared by ball-milling MgD_2 under 8 bar deuterated ammonia (ND_3). The milling treatment was applied for 12 h and a planetary ball mill (Fritsch P6) was used with a homemade steel jar designed for reactive ball milling at a revolution speed of 600 rpm. (Ball to power ratio of 5:1) The obtained nanocrystalline material was annealed at 300 °C under 8 bar of deuterated ammonia. Preliminary structural investigations were performed using in-house equipment with a Philips X'Pert X-ray diffractometer using Cu Kα radiation. The powder was spread onto a silicon single crystal and sealed in the glovebox with an airtight hood of Kapton foil. For caloric measurements a high pressure differential scanning calorimeter (Netzsch HP-DSC 204 Phoenix) was used. Neutron diffraction has been performed on the 2-axis diffractometer D20 at the high flux reactor of the Institut Laue-Langevin, Grenoble, France.[22] D20 is equipped with a curved linear position sensitive detector (PSD) resulting in rapid and simultaneous data acquisition over an angular range from 5 to 140° (2θ). Using a high resolution configuration with a germanium monochromator at high takeoff angle of 118° and a wavelength of 1.868 Å from its (115) reflection, a *d*-spacing range of 1−21 Å is covered with a time-resolution of 2 min per pattern. Data sets were corrected for detector efficiency, using LAMP[23,24] and employing a 2θ detector scan from a mostly incoherently scattering vanadium sample. Rietveld refinement was performed using the MAUD software.[25,26] The instrument function of the diffractometer was determined using crystalline silicon as a standard. During the fit this function is convolved with further line broadening because of reduced crystallite size and lattice strain and applied to each peak profile of phase specimen. A sample of deuterated magnesium amide was loaded in a can of ASI-316 L steel connected to a homemade high pressure rig. In particular the closed apparatus allowed a partial ammonia backpressure because of decomposition inside the sample holder, which proved beneficial for avoiding the full decomposition to nitride.[27]

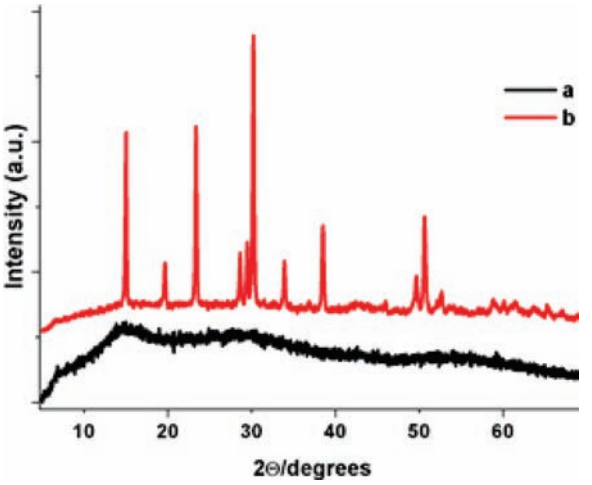

Figure 1. Comparison of different X-ray (Cu radiation) diffraction patterns. The starting material (MgD_2 ball milled under deuteraded ammonia) is in black, line a. The material after annealing at 300 °C is in red, line b.

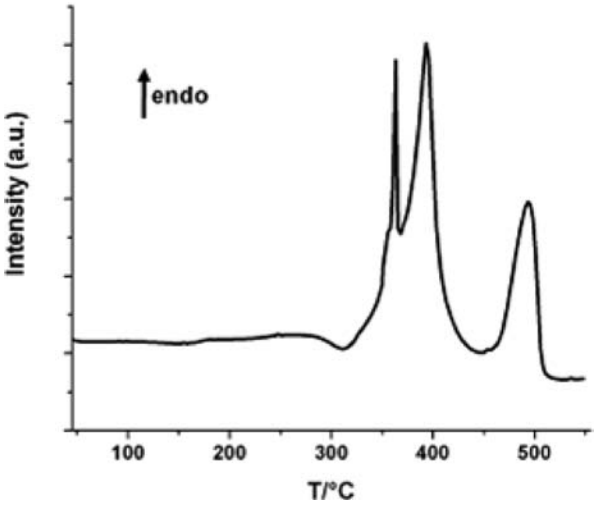

Figure 2. DSC trace for MgH_2 ball milled under ammonia. The heating ramp was 5 K/min under a 3 bar helium atmosphere.

3. Results

3.1. Preparation of $Mg(ND_2)_2$. After ball milling, $Mg(ND_2)_2$ appears to be nanocrystalline and no crystalline reflections can be seen in the X-ray diffraction pattern. (see Figure 1). Subsequent annealing under ND_3 atmosphere (8 bar) at 300 °C yielded crystalline $Mg(ND_2)_2$ for the in situ neutron diffraction measurements.

Throughout the paper, the material will be denoted as $Mg(NH_2)_2$ and MgNH under the assumption that the

(20) Jacobs, H.; Juza, R. *Z. Anorg. Allg. Chem.* **1969**, *370*, 248–253.
(21) Leng, H. Y.; Ichikawa, T.; Hino, S.; Hanada, N.; Isobe, S.; Fujii, H. *J. Power Sources* **2006**, *156*, 166–170.
(22) Hansen, T. C.; Henry, P. F.; Fischer, H. E.; Torregrossa, J.; Convert, P. *Meas. Sci. Technol.* **2008**, *19*, 034001.
(23) *LAMP, the Large Array Manipulation Program*; http://www.ill.eu/instruments-support/useful-tools/lamp/.
(24) Richard, D.; Ferrand, M.; Kearley, G. J. *J. Neutron Res.* **1996**, *4*, 33–39.
(25) Lutterotti, L. *The MAUD Program*; http://www.ing.unitn.it/~maud/.
(26) Lutterotti, L. *Nucl. Instrum. Methods Phys. Res., Sect. B* **2010**, *268*, 334–340.
(27) Hino, S.; Ichikawa, T.; Kojima, Y. *J. Chem. Thermodyn.* **2010**, *42*, 140–143.

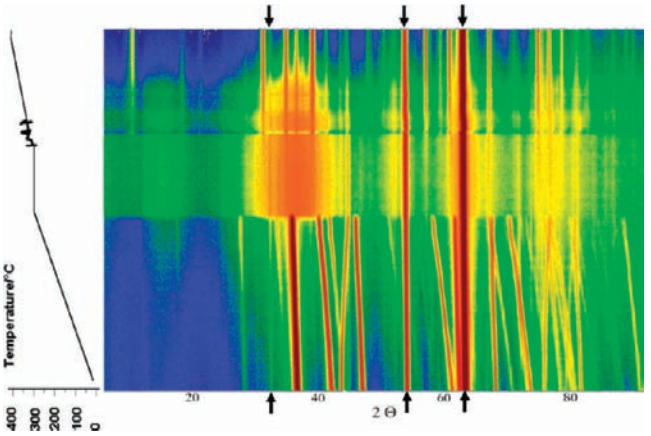

Figure 3. In situ neutron diffraction patterns for Magnesium amide decomposition. The arrows highlight the peaks coming from the steel sample container. It is possible to see how the cell parameters for magnesium amide are strongly influenced by the heating.

structural properties are very close to the deuterated $Mg(ND_2)_2$ and MgND. All neutron structural investigations have been performed on the deuterated materials.

3.2. DSC. The decomposition of ball milled magnesium amide was followed by DSC under helium atmosphere (Figure 2). One weak exothermic peak (minimum at ca. 315 °C) has its onset at around 270 °C and is followed by three intense endothermic events. Specifically, the first endothermic peak shows a maximum at around 360 °C and appears to be comparatively sharp. This is also partially overlapped to the tail of a second endothermic and broad peak with maximum at about 390 °C. Finally, at around 455 °C we see the onset of the third endothermic peak with its maximum at around 490 °C. As for the unambiguous assignment of these thermal events, unfortunately complete DSC literature data are missing for the system at hand so we refer to the diffraction patterns presented in Figures 1 and 3. The as milled product does not show evident Bragg peaks, suggesting that the material has a very small crystallite size or is an amorphous condition. Thus, we may ascribe the exothermic peak at around 300 °C to an amorphous-to-crystalline transformation or to a crystalline domain growth of ball milled $Mg(NH_2)_2$. Indeed, ex-situ X-ray diffraction of powder samples treated in the DSC up to 310 °C confirm the presence of crystalline magnesium amide. While the peak at 490 °C can be easily associated to the decomposition of MgNH to Mg_3N_2 (magnesium nitride), assignment of the decomposition of magnesium amide to magnesium imide to one thermal event out of the two present in the range 300−400 °C is not straightforward.[27] From the in situ measurements (see Figure 3) it appears that the two events belong to a deep structural modification process preceding the decomposition and to the decomposition process from $Mg(NH_2)_2$ to MgNH itself. We attribute the former process to the sharp peak overlapped by the broad decomposition feature.

3.3. In-Situ Neutron Diffraction. Figure 3 shows the neutron diffraction patterns obtained during heating magnesium amide from room temperature to 400 °C. In Figure 3 it is possible to notice the steel peaks from the sample holder, which are always present in the course of the treatment and subjected to just a small shift due to

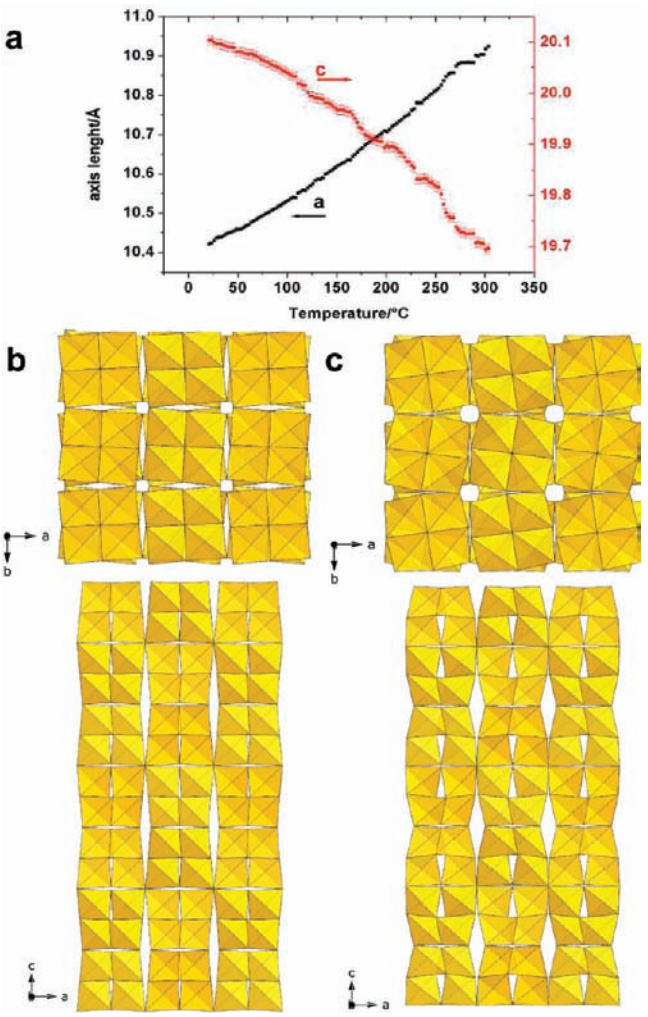

Figure 4. (a) Cell parameters for magnesium amide during the temperature ramp. (b) View perpendicular to the (001) direction (top) and perpendicular to the (010) direction (bottom) of the magnesium amide structure at room temperature. (c) View perpendicular to the (001) direction (top) and perpendicular to the (010) direction (bottom) of the magnesium amide structure before decomposition. For clarity only MgN_4 tetrahedra are shown.

thermal expansion. In contrast, the peaks associated to magnesium amide significantly shift as a function of temperature (Figure 3) and progressively change their intensity before disappearing at around 310 °C. At this temperature the material is subjected to a heavy transformation process, and the diffraction pattern only shows a broad peak at around 35 degrees. Even before the transformation process, the structure of magnesium amide is strongly deformed during heating. In Figure 3 the incipient structural rearrangement is evident both in the peak intensity and in the location involving changes in unit cell parameters and nearest neighbor distances prior to the full transformation. Figure 4a shows the values for the cell parameters of magnesium amide during the heating process. It is possible to see how the shorter *a*-axis is increasing, while the longer *c*-axis is decreasing during the heat treatment. At room temperature, the structure of magnesium amide can be seen as a sequence of "super-tetrahedral cluster" units (i.e., an octahedral vacancy where non adjacent faces are covered by four MgN_4 tedrahedra, see Figure 4b) sharing only the external

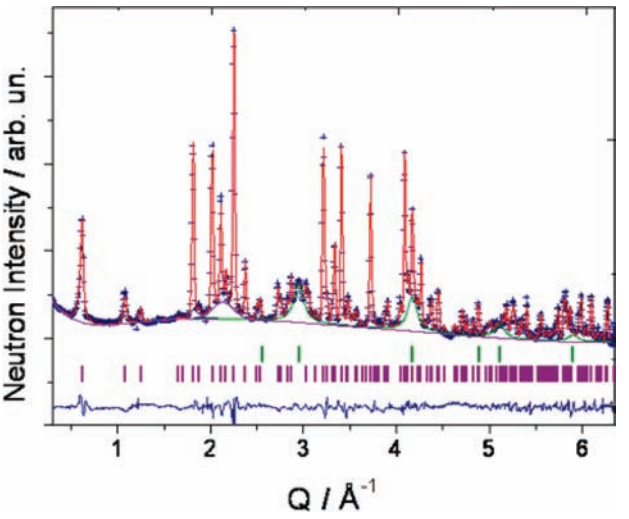

Figure 5. Rietveld refinement for the room temperature neutron diffraction pattern of MgNH. A vanadium sample holder was used. The red line is the calculated profile. The sequence of reflections from MgNH and MgO are given at the bottom of the picture.

vertex of the supertetrahedron, as in the case of beryllium amide ($Be(NH_2)_2$).[20] During the heating process these "supertetrahedral cluster" units are more and more distorted, with magnesium atoms moving away from each other, slowly altering the tetrahedral symmetry of the initial "supertetrahedral cluster". This results in an enlargement of the cavities surrounding each "supertetrahedral cluster" structural unit. It is evident that the strain associated to these deformations can not build up beyond a certain level; in fact at around 310 °C the material does not offer a structured diffraction pattern anymore, but only shows very broad peaks, which are likely to be associated with the melted state of magnesium amide. As the sample reaches 340 °C, the peaks expected for magnesium imide (Jacobs and Juza, PDF card 23−0391) start to appear with reflections getting stronger and sharper with increasing temperature. At 370 °C the formation of the imide is evident because of the presence of a distinctive peak at around 10.5 degrees. The obtained MgNH material was cooled down to room temperature, transferred to an argon glovebox and sealed in a vanadium can. A neutron diffraction pattern was collected at room temperature and used for structure determination.

3.4. Magnesium Imide Structure. In Figure 5 two types of reflection patterns can be distinguished: (i) broad peaks located approximately at 2.92, 4.16, and 5.22 Å^{-1} and (ii) a set of sharp reflections. The former peaks correspond fairly to a cubic phase modeled during refinement with periclase MgO. It may be surmised that this product of reaction is introduced in the powdered specimen during the various treatment stages to which it was subjected before being placed in the measurement cell. The low amount of this phase roughly evaluated in the neutron pattern suggests that this contribution can be minimized with a proper specimen handling. The second set of

Table 1. Refined Parameters for Magnesium Imide (MgNH) Obtained from Rietveld Refinement of Room Temperature Neutron Diffraction Data[a]

atom	label	Wyckoff position	*x*/*a*	*y*/*b*	*z*/*c*	Biso/Å^2
Mg	Mg1	6j	0.584(6)	0.8677(7)	0	0.8(1)
Mg	Mg2	6k	0.9285(7)	0.5721(6)	0.5	0.9(1)
N	N2	6j	0.6517(4)	0.7279(4)	0	0.68(7)
N	N1	6k	0.4954(4)	0.8633(4)	0.5	1.02(7)
D	H2	6j	0.9402(6)	0.745(6)	0	2.3(1)
D	H1	6k	0.4273(6)	0.7666(7)	0.5	3.1(2)

[a] Space group *P*6/*m* (175). Cell parameters: $a = b = 11.5796(3)$ Å and $c = 3.6811(1)$Å. $Z = 12$, $V = 427.463$ Å^3, $\rho = 1.833$ g/cm^3, weighted R pattern-Rwp% = 2.44, R pattern-Rp% = 1.77, GOF = 1.94.

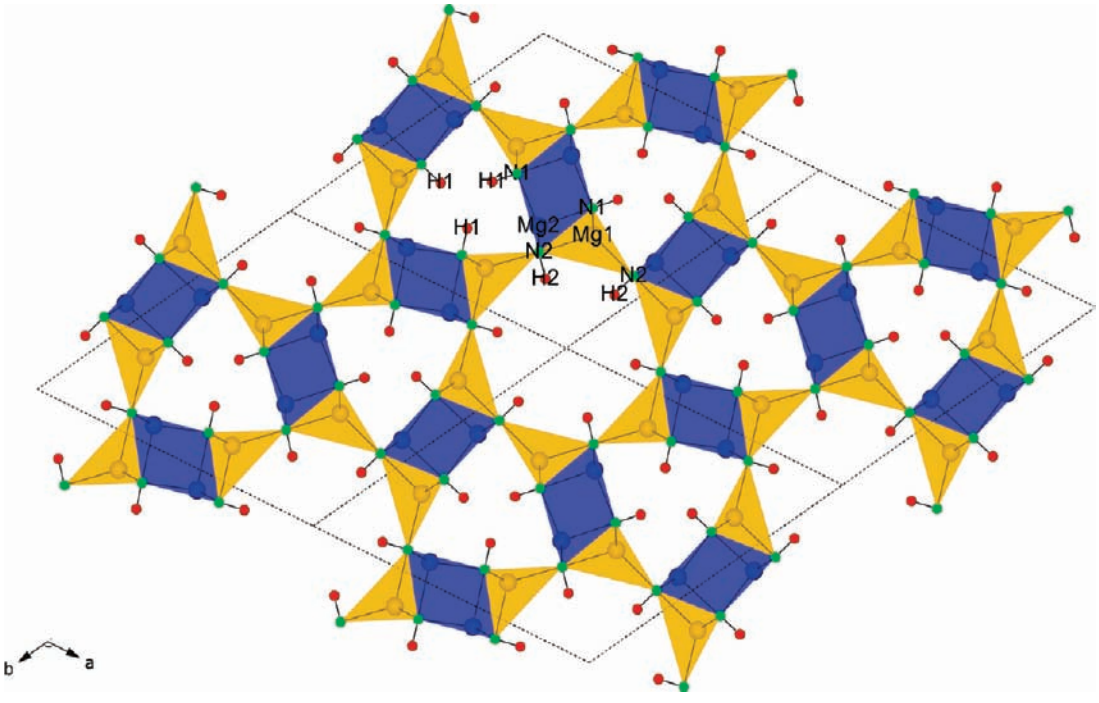

Figure 6. Structure representations of magnesium imide normal to the 001 plane. MgN4 tetrahedra are shown. The two non equivalent magnesium sites have been highlighted with yellow and blue color, respectively. Nitrogen atoms are in green. Deuterium atoms are red. The crystal cells are highlighted by the dotted line. Some atoms are labeled.

reflections was presumed to originate from MgNH. The first 20 peaks were selected manually, taking care to consider those with similar width. Such list was subjected to the indexing programs McMaille,[28] Dicvol,[29] and ITO.[30] All three converged in the output by proposing an hexagonal cell with lattice parameter $a = b = 11.567$ Å and $c = 3.683$ Å in reason of a combination of Rp, Figure of Merit, M(20) and F(20) parameters. A hexagonal cell of magnesium imide was indexed also by Jacobs and Juza[18] with lattice parameters $a = 11.574$ Å and $c = 3.681$ Å. They also reported picnometer density measurements of 1.837 g/cm^3. This information combined with the cell volume suggests that 12 MgNH units have to be considered in the structure solution. In fact, the density calculated assuming 12 MgNH units in the cell (Pearson code hP36) is 1.835 g/cm^3. Using Endeavor,[31] the space group giving a satisfactory solution to the neutron pattern was *P6/m*. After best fit using Endeavor on the first 25 reflections, the preliminary atomic coordinates and isotropic displacement parameters were established. These data were used as input in the Rietveld Refinement procedure. For the refinements, the presence of a cubic phase with lattice parameter $a = 4.247$ Å (MgO) was also taken into account. The results of the diffraction experiment together with the Rietveld analysis are shown in Figure 5.

4. Discussion

The structure of magnesium imide was confirmed to be hexagonal as already proposed by Juza et al.,[18] but with space group *P6/m* instead of P6322. The unit cell contains 12 MgNH formula units with magnesium, nitrogen, and hydrogen (deuterium) atoms in Wyckoff sites 6j and 6k. The structural solution is given in Table 1, and representations of the structure are shown in Figures 6 and 8a. The structure may be seen as a sequence of cyclosilicate-type 6-member rings of corner sharing MgN_4 tetrahedra superimposed to each other and connected by two edge sharing MgN_4 tetrahedra (see Figure 6). Also two types of voids can be distinguished along the *c*-direction: an hexagonal channel with a N−N diameter of approximately 7.34(5) Å and a triangular one with a N−N side of approximately 5.86(8)Å. The deuterium atoms are located inside these two types of cavities. In the MgNH structure, magnesium ions are always in a distorted tetrahedral coordination, with Mg−N distances ranging from 2.07(1)Å to 2.14(9)Å; slightly longer than in magnesium amide and magnesium nitride.[32,33] The angles range from 94.47° to 125.39°, showing a significant deviation from the ideal tetrahedral geometry. The minimum Mg−Mg distance is found for the edge sharing MgN_4 tetrahedra and is around 2.70(9)Å; similar to the shortest Mg−Mg distance in magnesium nitride, rather than the one reported for magnesium amide (around 3.40 Å).[32] In addition to the above-mentioned cavities, there are two main other cavities also defined by nitrogen atoms: one with an octahedral symmetry and another with a square based pyramid symmetry (see Supporting Information).

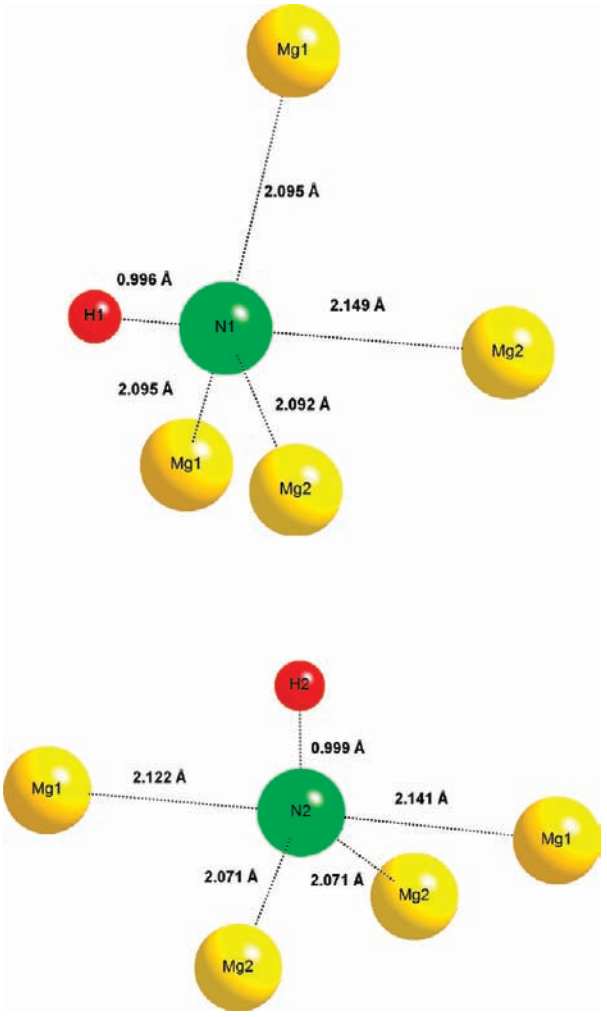

Figure 7. Nitrogen environment. The two inequivalent N1 and N2 atoms are shown. Distances between the nitrogen and the nearest neighbors are shown as dotted lines.

The two inequivalent nitrogen sites have both coordination five (see Figure 7) and are always surrounded by four magnesium atoms and one hydrogen atom. In the case of N1 the geometry adopted is a distorted trigonal bipyramid with one hydrogen and one magnesium atom in the apical positions (a trigonal pyramid configuration with a hydrogen atom in the apical position at the bottom). For N2, the geometry adopted is again trigonal bypiramid, but this time with a hydrogen atom in equatorial position and with magnesium atoms adopting a seesaw coordination around the nitrogen atom. The nitrogen-deuterium distances are of the order of 1.00 Å, well in agreement with other known alkali and alkaline earth imide structures. All the N−H groups point toward the hexagonal and triangular cavities (see Figures 6 and 8a), with hydrogen atoms H1 (always connected to N1 atoms) pointing toward the triangular cavities and with hydrogen atoms H2 (always connected to N2 atoms) pointing toward hexagonal cavities. This is in agreement with other known examples, such as $Li_2Mg(NH)_2$[12] or $Li_2Mg_2(NH)_3$[16] in which the -NH bonds are directed toward vacant sites. The distances between the closest hydrogen neighboring atoms range from around 2.60(7) Å in the hexagonal cavities to 1.94(7) Å in the triangular ones.

(28) Bogdanovic, B.; Schwickardi, M. *J. Alloys Compd.* **1997**, *253−254*, 1–9.
(29) Louer, D.; Boultif, A. *Z. Kristallogr.* **2006**, *1*, 225–230.
(30) Visser, J. W. *J. Appl. Crystallogr.* **1969**, *2*, 89–95.
(31) *Endeavour*; http://www.crystalimpact.com/endeavour/.
(32) Sorby, M. H.; Nakamura, Y.; Brinks, H. W.; Ichikawa, T.; Hino, S.; Fujii, H.; Hauback, B. C. *J. Alloys Compd.* **2007**, *428*, 297–301.
(33) Reckeweg, O.; DiSalvo, F. J. *Z. Anorg. Allg. Chem.* **2001**, *627*, 371–377.

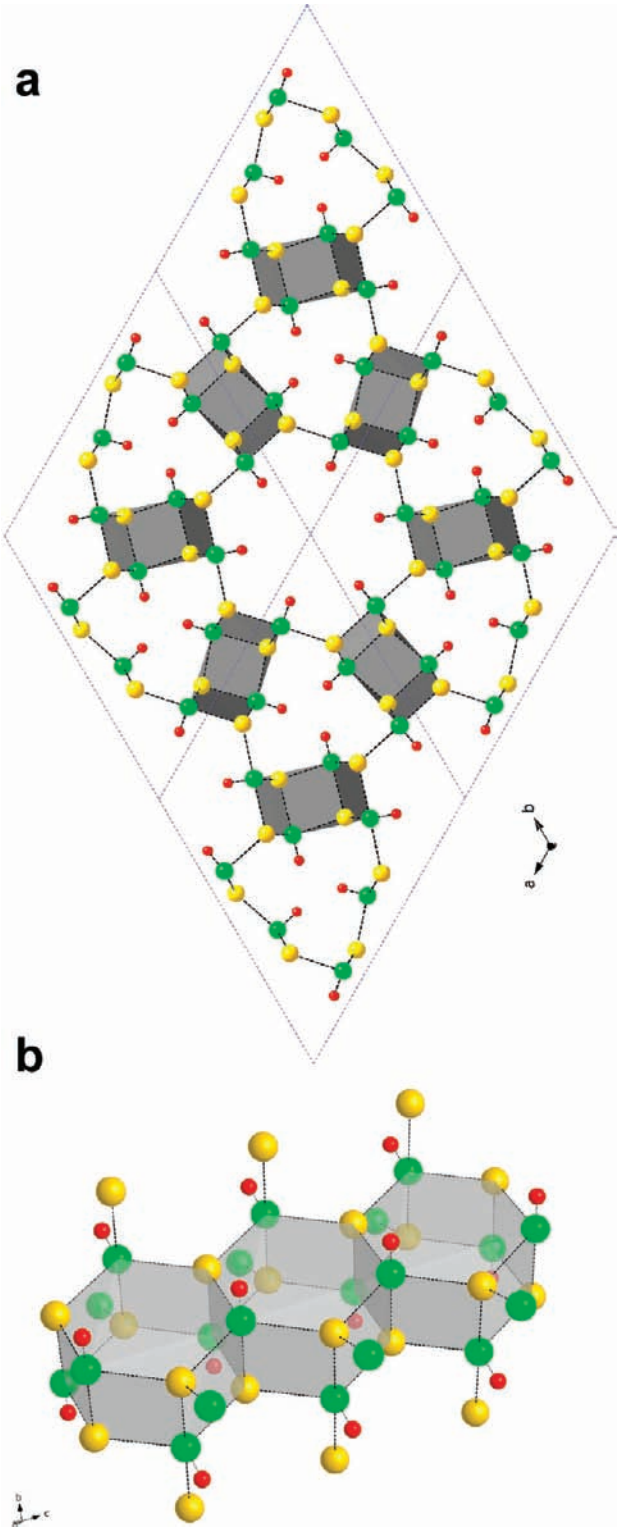

Figure 8. (a) Structure representations of magnesium imide normal to the 001 plane. The crystal cell is highlighted by the dotted line. (b) A small part (three units) of the infinite sequence of face sharing Mg_6N_6 units. Mg_6N_6 hexagonal prisms are highlighted in gray. Magnesium atoms are in yellow. Nitrogen atoms are in green. Deuterium atoms are red.

A strong similarity can be noticed between the solid state structure of MgNH described above and molecular magnesium imide compounds whose structure and reactivity have been extensively investigated in the past two decades.[34−39] Magnesium atoms present in such compounds always have a tetrahedral coordination. In particular, the $[(thf)MgNPh]_6$ compound synthesized by Hascall et al.[34] shows a slightly distorted hexagonal prismatic geometry for a Mg_6N_6 magnesium−nitrogen framework. This unit can be detected in MgNH as well (see Figure 8a and b). In the case of MgNH every magnesium atom is surrounded by nitrogen atoms and vice versa, while in $[(thf)MgNPh]_6$ magnesium and nitrogen atoms are also connected to oxygen or carbon atoms of the tetrahydrofuran (thf) and phenyl (Ph) ligands, respectively. In the case of MgNH the hexagonal prismatic structural units are forming, along the *c*-axis, linear chains composed by monomeric units connected to each other by sharing two faces, without the help of any ligand, as it is in the case of $[(thf)MgNPh]_6$.

The structure of magnesium imide is unique among the known alkaline earth imide compounds[40−43] and offers structural features nearer to cyclosilicate class rather than group II oxides. In particular, the analogy usually drawn between alkali and alkali earth oxides and corresponding imides does not hold for magnesium imide, which, at room temperature, has a completely different structure from magnesium oxide.

5. Conclusions

In summary in situ diffraction techniques allowed for the first time to achieve the direct synthesis and subsequent structural characterization of magnesium imide, a delicate decomposition product of magnesium amide. In-situ neutron diffraction evidenced also a significant structural rearrangement of magnesium amide (with the loss of long-range order) preceding its decomposition to magnesium imide. It is interesting to note that the solid state hydrogen storage system $Mg(NH_2)_2/2LiH$ does not show reasonable kinetic performances for temperatures below 180 °C; at that temperature the magnesium amide lattice is already deformed and noticeable differences are present with respect to the room temperature material (see Figure 4c). This suggests the presence of a specific potential barrier for hydrogen desorption which is overcome only when the structure of magnesium amide reaches a certain configuration.

Magnesium imide has a unique beryl-reminiscent porous structure, which can also be seen as a sequence of linked linear chains of face sharing Mg_6N_6 hexagonal prism clusters forming a kagome net. These building blocks resemble the units that are found for molecular magnesium imide compounds. The specific properties of this material are at present

(34) Hascall, T.; Ruhlandt-Senge, K.; Power, P. P. *Angew. Chem., Int. Ed. Engl.* **1994**, *33*, 356–357.
(35) Grigsby, W. J.; Power, P. P. *Dalton Trans.* **1996**, 4613–4615.
(36) Grigsby, W. J.; Hascall, T.; Ellison, J. J.; Olmstead, M. M.; Power, P. P. *Inorg. Chem.* **1996**, *35*, 3254–3261.
(37) Rood, J. A.; Noll, B. C.; Henderson, K. W. *Inorg. Chem.* **2007**, *46*, 7259–7261.
(38) Rood, J. A.; Hinman, S. E.; Noll, B. C.; Henderson, K. W. *Eur. J. Inor. Chem.* **2008**, *25*, 3935–3942.
(39) Hascall, T.; Olmstead, M. M.; Power, P. P. *Angew. Chem., Int. Ed. Engl.* **1994**, *33*, 1000–1001.
(40) Sichla, T.; Jacobs, H. *Z. Anorg. Allg. Chem.* **1996**, *622*, 2079–2082.
(41) Wegner, B.; Essmann, R.; Jacobs, H.; Fischer, P. *J. Less Common Met.* **1990**, *167*, 81–90.
(42) Jacobs, H.; Niewa, R.; Sichla, T.; Tenten, A.; Zachwieja, U. *J. Alloys Compd.* **1997**, *246*, 91–100.
(43) Brese, N. E.; O'Keeffe, M.; Von Dreele, R. B. *J. Solid State Chem.* **1990**, *88*, 571–576.

unknown, but possible applications can range from separation adsorption to catalysis.

Acknowledgment. Part of this work was carried on within the European Commission Sixth Framework Programme under the Marie Curie Research Training Network COSY (Contract No. MRTN-CT-2006-035366) and the Integrated Project NESSHY. The authors thank also Dr. Maria Orlova for the help provided during diffraction measurements. We thank also the reviewers for their helpful comments.

Supporting Information Available: Further details on material structure, decomposition process, and X-ray crystallographic file (CIF). This material is available free of charge via the Internet at http://pubs.acs.org.